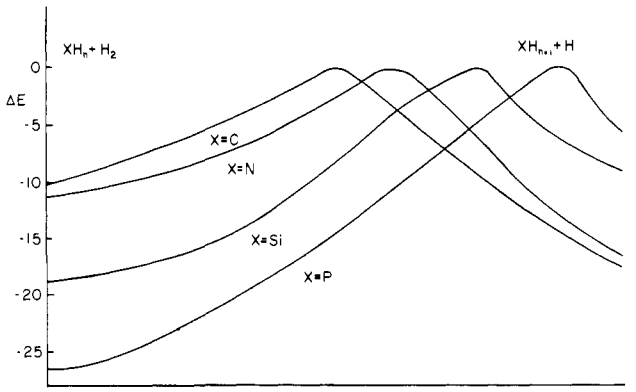

Figure 4. Schematic of POL-CI potential energy curves. The zero of energy is arbitrarily taken to be the transition state in each curve. The position of the transition state along the "reaction path" is determined by the relative bond length changes in Table I.

Table X. CPU Time Comparisons for CH_5[a]

method[b]	time,[c] min	method[b]	time,[c] min
RHF/6-31G*	8	UMP3/6-311G*	28
UHF/6-31G*	4	UMP3/6-31G**	64
UMP3/6-31G*	11	UMP3/6-311G**	130
POL-CI/6-31G*	30		

[a] All calculations were performed on an IBM 370/158. [b] The RHF- and UHF-based calculations were carried out with ALIS and GAUSSIAN80, respectively. [c] All times are cumulative.

to be a small MCSCF augmented by POL-CI. Thermodynamic differences, and therefore relative barriers, appear to be predicted equally well by Møller–Plesset methods.

Errors in the predicted energetics can arise from deficiencies in both the basis sets and computational levels. Since the predicted thermodynamic ΔE's appear to be in reasonable agreement with available experimental results, it is most important to estimate errors in the POL-CI/6-31G* barriers. Walch[4] has estimated that his value of 15.9 kcal/mol for the H + CH_4 barrier is close to the basis set limit for POL-CI and, using the H + H_2 reaction, estimates the POL-CI error to be about 2.4 kcal/mol. Since the POL-CI/6-31G* barrier for the same reaction is 17.6 kcal/mol, one can estimate a 4.1 kcal/mol error for this level of theory, approximately equally split between basis set and methodology. If similar errors (~4 kcal/mol) apply to the other three systems treated here, then the H_2 + XH_n barriers would be reduced to 15.2, 7.2, and 22.2 kcal/mol, respectively, for X = Si, N, and P. The barriers for the reverse reactions would concomitantly be reduced to 5.3, 13.6, and 1.6 kcal/mol. The latter is consistent with point 2 above.

Regarding the third point listed above, it is useful to consider Table X in which the 370/158 computer times required for the various methods are compared for CH_5. These times are not directly comparable, since they arise from two rather different sets of codes (GAUSS80 vs. ALIS). Nonetheless, they do provide some sense for the relative times required to carry out these calculations. For the same basis set (i.e., 6-31G*) UMP3 is apparently much faster than POL-CI; however, this must be viewed in the context of the relative accuracy of the calculations. To obtain barriers at the UMP3 level which are comparable with the POL-CL results requires the use of 6-31G** or 6-311G** basis sets (cf. Tables II–IV). This makes the POL-CI approach more desirable if these comparisons hold up for more complex systems. On the other hand, it should also be noted that for transition states which do not have linear or nearly lnear X···H···Y structures, the choice of reference configurations in the MCSCF may be more complicated, and this may raise the number of configurations and time required in the POL-CI step. Finally, as noted above, UMP3 and POL-CI do predict comparable *relative* barriers at the same basis set level, and this will clearly increase in importance as the sizes of the molecules increase.

Acknowledgment. This work was supported by the donors of the Petroleum Research Fund, administered by the Americal Chemical Society. The computer time made available by the North Dakota State University Computer Center is gratefully acknowledged, as are very helpful discussions with Professor R. D. Koob and Mr. Clayton George. Finally, the authors are particularly grateful to Professor S. Topiol for making the IBM version of GAUSSIAN80 available and Professor K. Ruedenberg and his group for their generosity in giving us a copy of ALIS.

Registry No. CH_3, 2229-07-4; SiH_3, 13765-44-1; NH_2, 13770-40-6; PH_2, 13765-43-0; H_2, 1333-74-0.

Experimental and Theoretical Investigations of the Unimolecular Dissociation of Nascent Ion–Molecule Clusters: $H_2O{\cdot}H_3O^+$, $NH_3{\cdot}NH_4^+$, and $CO_2{\cdot}CO_2^+{\cdot}$

A. J. Illies, M. F. Jarrold, L. M. Bass,† and M. T. Bowers*

Contribution from the Department of Chemistry, University of California, Santa Barbara, California 93106. *Received February 28, 1983*

Abstract: The metastable fragmentation of three nascent gas-phase ion–molecule collision complexes, $H_2O{\cdot}H_3O^+$, $NH_3{\cdot}NH_4^+$, and $CO_2{\cdot}CO_2^+{\cdot}$, has been studied using mass-analyzed ion kinetic energy spectrometry (MIKES). The clusters were formed in an ion source which was cooled to promote the association reactions. The kinetic energy release distributions and the metastable intensities were measured as a function of the ion source pressure. The metastable fragmentation was modeled using statistical phase space theory. The experimental data and theoretical results suggest that a single collision between the nascent cluster and a molecule is sufficient to quench the unimolecular reaction.

I. Introduction

Studies of proton-bound dimers and ionic clusters by high-pressure mass spectrometry and ion cyclotron resonance spectrometry have resulted in a thorough understanding of the thermodynamics and kinetics of formation for many ion–molecule clusters.[1-5] The motive behind the intense research in this area

† Present Address: Department of Chemistry, University of Warwick, Coventry, CV4 7AL, UK.

(1) P. Kebarle, *Annu. Rev. Phys. Chem.*, **28**, 445 (1977).
(2) M. Meot-Ner in "Gas Phase Ion Chemistry", Vol. 1, M. T. Bowers, Ed., Academic Press, New York, 1979.

0002-7863/83/1505-5775$01.50/0

is the role that clustering plays in the earth's atmosphere, interstellar clouds, nucleation, solvation, and vapor-to-liquid transition.[1,6,7] The mechanism for production of ion–molecule clusters is illustrated in the following scheme, where the ion A^+ is usually formed by electron impact (EI) in the laboratory:

$$A^+ + A \rightleftarrows AA^{+*} \quad (1a)$$

$$AA^{+*} + M \rightarrow AA^+ + M \quad (1b)$$

Formation of proton-bound dimers requires an additional step:

$$A^+ + A \rightarrow AH^+ + (A\text{–}H) \quad (2a)$$

$$AH^+ + A \rightleftharpoons AHA^{+*} \quad (2b)$$

$$AHA^{+*} + M \rightarrow AHA^+ + M \quad (2c)$$

The kinetics and especially the equilibria of cluster and proton-bound dimer formation have been extensively studied. Equilibrium constant measurements as a function of temperature yield ΔH and ΔS of reaction.[1,2,5]

Although association reactions have been studied since the early 1960s,[8] resulting in a wealth of information, it is only recently that the metastable reactions of association products have drawn considerable interest. McLuckey and co-workers[9] recently studied the metastable decompositions as well as collision-induced dissociation (CID) of a series of organic mixed proton-bound dimers via the reactions:

$$AHB^+ \rightarrow AH^+ + B \quad (3)$$

$$AHB^+ \rightarrow BH^+ + A \quad (4)$$

The ratios of AH^+ to BH^+ intensities in these experiments were correlated with the ratios of the proton affinities of the neutrals. Sunner and Kebarle have also investigated the metastable reactions of cluster ions;[10] this work, however, was directed toward the effect that metastable decomposition has on the measurement of ion–molecule association equilibria rather than a study of the metastable decompositions themselves.

Recently, studies of the unimolecular decomposition, CID, and photoionization of small molecular clusters formed in supersonic molecular beams have drawn considerable interest.[11-17] In these experiments, the cluster ions are formed by a different mechanism. Neutral van der Waals clusters are formed in a supersonic expansion, and then ionized either by electron impact or by photoionization. Using electron impact ionization of clusters formed in a supersonic nozzle, Futrell et al.[16] investigated the metastable and collision-induced dissociation of CO_2 and NH_3 cluster ions. They did not observe metastable dissociation for $CO_2{\cdot}CO_2^{+\cdot}$ or $NH_3{\cdot}NH_4^+$. Stace and Shukla[14] in a similar experiment measured the average kinetic energy release for the unimolecular decomposition of $(CO_2)_n^{+\cdot}$ for $n = 3$ to 13; however, they did not report any results for $n = 2$.

In this paper we report the results of studies on the metastable decomposition of $H_2O{\cdot}H_3O^+$, $NH_3{\cdot}NH_4^+$ and $CO_2{\cdot}CO_2^{+\cdot}$. The specific reaction sequences are given in eq 5–7.

$$H_2O^{+\cdot} + H_2O \rightarrow H_3O^+ + OH\cdot \quad (5a)$$

$$H_3O^+ + H_2O \rightarrow H_2O{\cdot}H_3O^{+*} \quad (5b)$$

$$H_2O{\cdot}H_3O^{+*} \xrightarrow{M} H_2O{\cdot}H_3O^+ \quad (5c)$$

$$H_2O{\cdot}H_3O^{+*} \rightarrow H_3O^+ + H_2O \quad (5d)$$

$$NH_3^{+\cdot} + NH_3 \rightarrow NH_4^+ + NH_2\cdot \quad (6a)$$

$$NH_4^+ + NH_3 \rightarrow NH_3{\cdot}NH_4^{+*} \quad (6b)$$

$$NH_3{\cdot}NH_4^{+*} \xrightarrow{M} NH_3{\cdot}NH_4^+ \quad (6c)$$

$$NH_3{\cdot}NH_4^{+*} \rightarrow NH_4^+ + NH_3 \quad (6d)$$

$$CO_2^{+\cdot} + CO_2 \rightarrow CO_2{\cdot}CO_2^{+\cdot *} \quad (7a)$$

$$CO_2{\cdot}CO_2^{+\cdot *} \xrightarrow{M} CO_2{\cdot}CO_2^{+\cdot} \quad (7b)$$

$$CO_2{\cdot}CO_2^{+\cdot *} \rightarrow CO_2^{+\cdot} + CO_2 \quad (7c)$$

In the experiments reported in this paper, cluster formation and collisional stabilization of the excited association complex occur in a chemical ionization (CI) source. Unimolecular fragmentation takes place in the ion source as well as throughout the ion flight path to the detector. We have measured both the metastable peak shapes and the metastable to main beam intensity ratios as a function of the ion source pressure (which is related to the number of collisions which takes place in the ion source) for reactions 5d, 6d, and 7c. Kinetic energy release distributions were determined from the metastable peaks. Both the kinetic energy release distributions and the metastable to main beam intensity ratios were modeled using statistical phase space theory. Comparisons between the experimental and the theoretical results are presented.

II. Experimental Section

All experiments were performed using a reverse geometry mass spectrometer (V.G. Analytical, ZAB-2F) with a combined EI/CI temperature-variable ion source constructed at UCSB.[18] The ionizing electron energy was 150 eV. Experiments were performed as a function of reactant gas pressure over the range from 0.003 to 0.015 torr. The ion exit slit was 0.15 mm × 6.3 mm. The sample gas pressure was measured with a capacitance manometer (MKS Baratron, Model 170M). Ion source residence time distributions were measured by pulsing the ionizing electron beam and measuring the ion arrival time distribution at the detector using the method of Sroka et al.[19] With the ion source conditions described above, and assuming a Langevin collision rate, the average number of collisions in the ion source between the cluster ions and the neutral gas is estimated to vary between ~0.5 and ~12 over the experimental pressure range. The ion source was cooled in order to promote the clustering reactions being studied.[1,5,20-22]

The metastable fragmentations were studied using mass-analyzed ion kinetic energy spectrometry (MIKES).[18,23] The ion accelerating voltage was 8 kV. The background pressure in the second field-free region (2-FFR), where the metastable reactions of interest occur, was $\leq 1.5 \times 10^{-9}$ torr as indicated on an ion gauge mounted at the entrance to one of the diffusion pumps. CID measurements were carried out by admitting helium into the collision cell located at the focal point in the 2-FFR of the mass spectrometer. These CID experiments were carried out to ensure that the processes studied were true metastable reactions

(3) D. Smith and N. G. Adams in "Gas Phase Ion Chemistry", Vol. 1, M. T. Bowers, Ed., Academic Press, New York, 1979.
(4) L. M. Bass, P. R. Kemper, V. G. Anicich, and M. T. Bowers, *J. Am. Chem. Soc.*, **103**, 5283 (1981).
(5) J. V. Headley, R. S. Mason, and K. R. Jennings, *J. Chem. Soc., Faraday Trans. 1*, **78**, 933 (1982).
(6) W. T. Huntress and G. F. Mitchell, *Ap. J.*, **231**, 456 (1979).
(7) A. W. Castlemann in "Kinetics of Ion-Molecule Reactions", P. Ausloos, Ed., Plenum, New York, 1979.
(8) M. S. B. Munson, F. H. Field, and J. L. Franklin, *J. Chem. Phys.*, **37**, 1790 (1962).
(9) S A. McLuckey, D. Cameron, and R. G. Cooks, *J. Am. Chem. Soc.*, **103**, 1313, (1981).
(10) J. Sunner and P. Kebarle, *J. Phys. Chem.*, **85**, 327 (1981).
(11) H. Helm, K. Stephan, and T. D. Mark, *Phys. Rev. A*, **19**, 2154 (1979).
(12) A. J. Stace and A. K. Shukla, *Int. J. Mass Spectrom. Ion Phys.*, **36**, 119 (1980).
(13) A. J. Stace and A. K. Shukla, *J. Phys. Chem.*, **86**, 865 (1982).
(14) A. J. Stace and A. K. Shukla, *Chem. Phys. Lett.*, **85**, 157 (1982).
(15) K. Stephan and T. D. Mark, *Chem. Phys. Lett.*, **87**, 226 (1982).
(16) J. H. Futrell, K. Stephan, and T. D. Mark, *J. Chem. Phys.*, **76**, 5893 (1982).
(17) A. J. Stace and A. K. Shukla, *J. Am. Chem. Soc.*, **104**, 5314 (1982).
(18) M. F. Jarrold, A. J. Illies, and M. T. Bowers, *Chem. Phys.*, **65**, 19 (1982).
(19) G. Sroka, C. Chang, and G. G. Meisels, *J. Am. Chem. Soc.*, **94**, 1052 (1972).
(20) F. E. Niles and W. W. Robertson, *J. Chem. Phys.*, **42**, 3277 (1965).
(21) D. K. Bohme, D. B. Dunkin, F. C. Fehsenfeld, and E. E. Ferguson, *J. Chem. Phys.*, **51**, 863 (1969).
(22) D. A. Durden, P. Kebarle, and A. Good, *J. Chem. Phys.*, **50**, 805 (1969).
(23) R. G. Cooks, J. H. Beynon, R. M. Caprioli, and G. R. Lester, "Metastable Ions", Elsevier, Amsterdam, 1973.

and were not due to collision-induced dissociation with the background gas in the 2-FFR. In all cases metastable and collision-induced processes could be differentiated by the differences in kinetic energy release.

The ratios of the metastable to main beam intensities were determined from the peak heights recorded using single-scan analog recording with both the mass spectrometer source and collector slits open.[24] The kinetic energy release distributions were derived from the metastable peaks which were recorded using high-energy resolving power (~15 000 fwhm). Because of the weak signal intensity under these conditions, the metastable peaks were recorded using single ion counting techniques and the data were accumulated in a multichannel analyzer.[18] The water used was outgassed deionized water; the ammonia (99.99%) and the CO_2 (99.99%) were both supplied by Linde.

III. Results and Discussion

A. Experiment. 1. Metastable to Main Beam Intensity Ratio. Metastable and main beam peaks were recorded over the ion source pressure range 0.001–0.015 torr. The relative metastable intensities, obtained from the metastable and main beam peak heights, are shown in Figure 1 for the unimolecular fragmentation of $H_2O{\cdot}H_3O^+$, $NH_3{\cdot}NH_4^+$, and $CO_2{\cdot}CO_2^{+}\cdot$. Figure 1 shows that as the ion source pressure is increased, the relative metastable intensity decreases. This result is exactly what one would expect since as the ion source pressure is raised, the amount of collisional stabilization increases. It should be noted, however, that as the *relative* metastable intensity decreases with pressure, the *absolute* metastable intensity increases over the pressure range studied owing to the increase in the cluster ion main beam intensity.

2. Kinetic Energy Release Distributions. Kinetic energy release distributions were derived from the metastable peak shapes measured in a separate set of experiments in which high-energy resolving power (~15 000 fwhm) was used. Under these conditions, the main beam peak was much narrower than the metastable peak and the kinetic energy release distribution could be determined from the metastable peak without making corrections for the main beam energy distribution. The distributions were obtained by drawing a smooth curve through the metastable peak followed by numerical differentiation.[24,25]

Figure 2 shows the kinetic energy release distributions obtained for the metastable decomposition of $H_2O{\cdot}H_3O^+$, $NH_3{\cdot}NH_4^+$, and $CO_2{\cdot}CO_2^{+}\cdot$. For $CO_2{\cdot}CO_2^{+}\cdot$ two data sets are shown in Figure 2 to give an indication of the reproducibility of the kinetic energy release distributions derived from independent measurements. The average kinetic releases determined from the distributions were 1.9 meV for $H_2O{\cdot}H_3O^+$, 1.3 meV for $NH_3{\cdot}NH_4^+$, and 1.6 meV for $CO_2{\cdot}CO_2^{+}\cdot$. Note that these metastable reactions result in a very small kinetic energy release. The small kinetic energy release in these reactions implies that the reverse activation barrier is negligible.

The kinetic energy release distributions were found to be independent of the ion source pressure. This result can be understood by reference to reactions 5 through 7 depicting the processes which are being studied. If it is assumed that only one collision is required to remove the excess internal energy (unit stabilization efficiency), then the ions which undergo a collision will no longer be able to contribute to the metastable intensity. Conversely, only those ions which exit the ion source without having undergone a collision are able to undergo metastable fragmentation.

In the Introduction it was noted that Futrell et al.[16] and Stace and Shukla[12] did not observe unimolecular decomposition for $NH_3{\cdot}NH_4^+$ [16] or $CO_2{\cdot}CO_2^{+}\cdot$ [12,16] when the ions were formed in a supersonic molecular beam. In the work reported here, we observed the unimolecular reactions of $NH_3{\cdot}NH_4^+$, $H_2O{\cdot}H_3O^+$, and $CO_2{\cdot}CO_2^{+}\cdot$ following cluster formation by ion–molecule reactions.[5-7] As was stated in the Experimental Section, we carried out both metastable and CID experiments in order to prove that the reactions being investigated were unimolecular and not collision-induced by the background gas. There are three possible

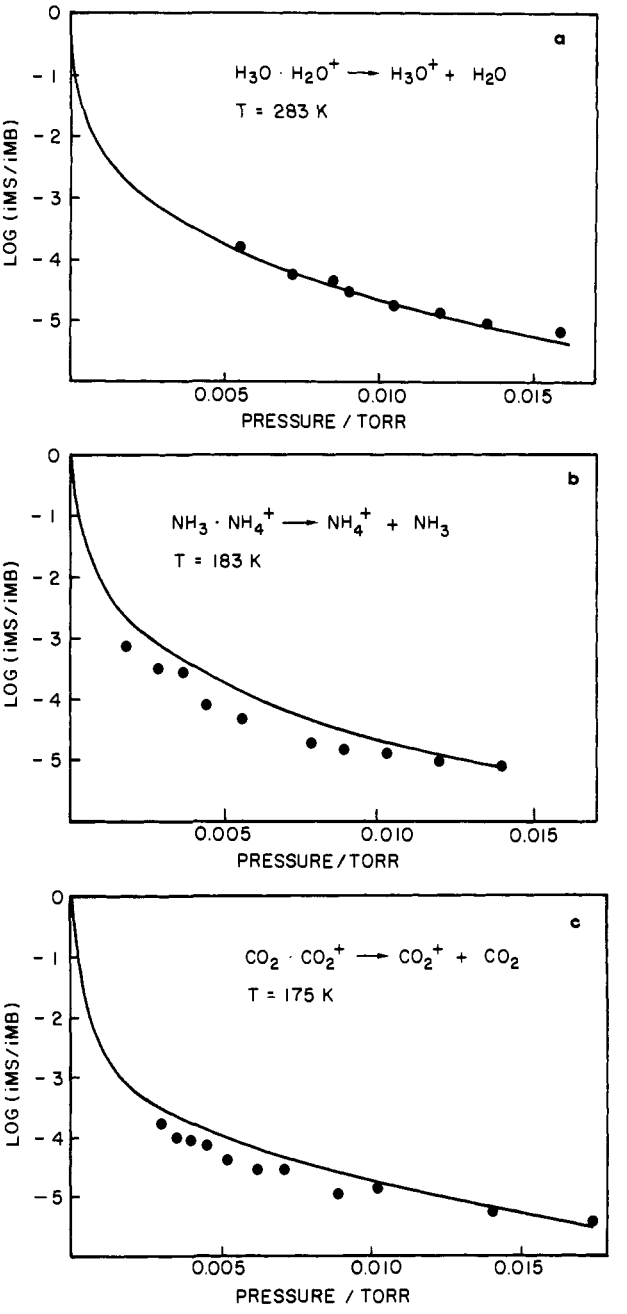

Figure 1. Metastable to main beam intensity ratio as a function of ion source pressure for the reactions: (a) $H_2O{\cdot}H_3O^+ \rightarrow H_3O^+ + H_2O$, (b) $NH_3{\cdot}NH_4^+ \rightarrow NH_4^+ + NH_3$, and (c) $CO_2{\cdot}CO_2^{+}\cdot \rightarrow CO_2^{+}\cdot + CO_2$. The points are the experimental data and the solid lines are the results of statistical phase space theory calculations.

explanations for the apparent discrepancy between our results and those of Futrell et al. and Stace and Shukla.

(a) The ion clusters are formed by different processes and therefore the internal energy and angular momentum distributions may be different. The neutral clusters formed in a supersonic nozzle will be rotationally and vibrationally cold. After electron impact ionization, the ions' vibrational distribution will be governed by the Franck–Condon factors while the rotational distribution will remain essentially the same as that of the neutral clusters. In the experiments reported here, the cluster ions were generated by an association reaction. Thus the energy distributions and angular momentum distribution will be determined by the collision forming the cluster and the distributions will be larger than thermal.

(b) The ions in the molecular beam may undergo stabilizing collisions before being extracted from the high-pressure region. (In this work we conclude that just one ion–neutral collision is

(24) A. J. Illies, M. F. Jarrold, and M. T. Bowers, *J. Am. Chem. Soc.*, **104**, 3587 (1982).

(25) M. F. Jarrold, A. J. Illies, N. J. Kirchner, W. Wagner-Redeker, M. T. Bowers, M. L. Mandich, and J. L. Beauchamp, *J. Phys. Chem.*, **87**, 2213 (1983).

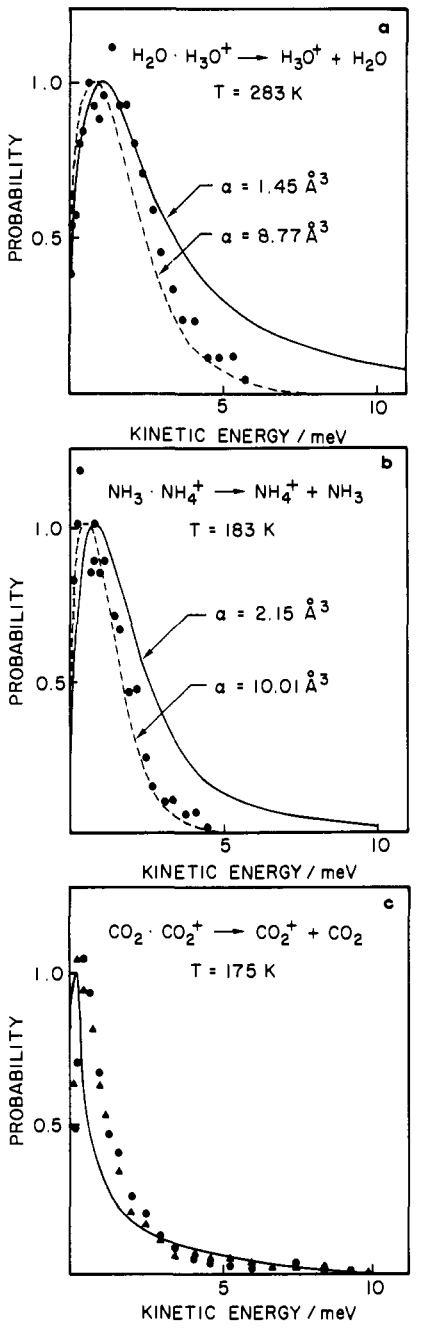

Figure 2. Metastable kinetic energy release distributions for the reactions: (a) $H_2O \cdot H_3O^+ \rightarrow H_3O^+ + H_2O$, (b) $NH_3 \cdot NH_4^+ \rightarrow NH_4^+ + NH_3$, and (c) $CO_2 \cdot CO_2^{+\cdot} \rightarrow CO_2^{+\cdot} + CO_2$. The points are the experimental data and the lines are the results of statistical phase space theory calculations.

enough to quench the metastable reaction.)

(c) In the molecular beam experiments, the unimolecular product intensity may be too weak to be observed relative to the collision-induced product intensity.

Although all three explanations given above are reasonable, the last one deserves more attention. In the experiments of Futrell et al., the existence of metastable reactions was inferred by a long extrapolation in a plot of the product intensity vs. the pressure in the analysis region (1-FFR). The lowest pressure at which measurements were made was approximately 4×10^{-5} torr. In the present work the background pressure was less than 2×10^{-9} torr in the analysis region (2-FFR) and the collision-induced component was very small.

B. Theoretical Results and Discussion. Ion–molecule association reactions have been the subject of a number of theoretical studies[26-30] including several from this laboratory.[29,30] One of the assumptions of the previous studies is that formation of the nascent cluster occurs at the collision rate. In view of the large number of simple ion–molecule reactions which are known to proceed at the collision rate, this is a reasonable assumption. The collision rate is determined by the flux through the orbiting transition state. If the rate of formation of the nascent complex is controlled by the orbiting transition state, then microscopic reversibility requires that the rate of the subsequent unimolecular reaction of the nascent complex is also controlled by the orbiting transition state. Thus the microcanonical rate constant for the unimolecular reaction of the nascent complex is given by[31]

$$k(E,J) = F^{\text{orb}}(E,J)/\rho(E,J) \tag{8}$$

where $F^{\text{orb}}(E,J)$ is the flux through the orbiting transition state and $\rho(E,J)$ is the density of states in the complex. If the rate is determined by the orbiting transition state, it is reasonable to assume that the kinetic energy release distribution will also be governed by the orbiting transition state. Hence the probability of kinetic energy release E_t for a given E,J state is[31]

$$P(E,J;E_t)\,dE_t = \frac{F^{\text{orb}}(E,J;E_t)\,dE_t}{F^{\text{orb}}(E,J)} \tag{9}$$

where $F^{\text{orb}}(E,J;E_t)$ is the flux through the orbiting transition state at product kinetic energy E_t.

For comparison with experiment, the equations discussed above must be averaged over the energy and angular momentum distributions sampled in the experiments. The equations required to evaluate the fluxes and densities of states have been reviewed by Chesnavich and Bowers.[32] All species except $CO_2^{+\cdot}$ and CO_2, which are linear, were treated as spherical tops, an approximation that introduces only a few percent error.[33] The input parameters used in the calculations are discussed in the Appendix. For the orbiting transition states, reliable values were available from the literature for all parameters. Parameters for the complexes are not so well known. However, values of ΔH and ΔS for the reactions are available from equilibrium measurements. ΔH can be used to evaluate the zero-point energy difference between the complex and products, and ΔS can be used as a guide for estimating the parameters of the complex which are the most uncertain. Specific details are given in the Appendix. An important feature of these calculations is that all parameters were selected prior to performing the calculations and were not adjusted to fit the experimental data.

Table I. Definition of Parameters Used in the Equations in the Text

t_r	ion source residence time
t_1	flight time to entry of the 2-FFR
t_2	flight time to exit of the 2-FFR
t_3	flight time to the detector
$k_1(E,J)$	unimolecular rate constant
k_2	bimolecular rate constant calculated from ADO theory[34]
[B]	neutral gas concentration in the ion source
$P(t_r)$	measured ion source residence time distribution
k_B	Boltzmann constant
T	ion source temperature

(26) W. N. Olmstead, M. Lev-On, D. M. Golden, and J. I. Brauman, *J. Am. Chem. Soc.*, **99**, 992 (1977).
(27) D. R. Bates, *J. Phys. B*, **12**, 4135 (1979).
(28) E. Herbst, *J. Chem. Phys.*, **72**, 5284 (1980).
(29) L. Bass, W. J. Chesnavich, and M. T. Bowers, *J. Am. Chem. Soc.*, **101**, 5493 (1979).
(30) L. M. Bass, R. D. Cates, M. F. Jarrold, N. J. Kirchner, and M. T. Bowers, *J. Am. Chem. Soc.*, in press.
(31) W. J. Chesnavich, L. Bass, T. Su, and M. T. Bowers, *J. Chem. Phys.*, **74**, 2228 (1981); M. F. Jarrold, L. M. Bass, P. R. Kemper, P. A. M. van Koppen, and M. T. Bowers, *ibid.*, **78**, 3756 (1983).
(32) W. J. Chesnavich and M. T. Bowers in "Gas Phase Ion Chemistry", Vol. I, M. T. Bowers, Ed., Academic Press, New York, 1979; W. J. Chesnavich and M. T. Bowers, *Prog. React. Kinet.*, **11**, 137 (1982).
(33) W. J. Chesnavich and M. T. Bowers, *J. Chem. Phys.*, **66**, 2306 (1977); W. J. Chesnavich, Ph.D. Thesis, Department of Chemistry, University of California, Santa Barbara, 1976.

1. Metastable to Main Beam Intensity Ratio. The detected main beam signal is composed of complexes which are stabilized by bimolecular collisions in the source and nascent complexes which reach the detector before dissociating. Assuming a single collision is sufficient for stabilization (unit stabilization efficiency), the microcanonical fraction stabilized is

$$F_S(E,J,t_r) = \frac{k_2[B]}{k_2[B] + k_1(E,J)}[1 - e^{-[k_1(E,J)+k_2[B]]t_r}] \quad (10)$$

and the fraction of nascent complexes reaching the detector is

$$F_D(E,J,t_r) = e^{-k_1(E,J)[t_r+t_3]}e^{-k_2[B]t_r} \quad (11)$$

The parameters used in the above and in subsequent equations are defined in Table I. The detected metastable signal is derived from complexes which fragment in the second field-free region which is given by

$$F_{MS}(E,J,t_r) = [e^{-k_1(E,J)[t_r+t_1]} - e^{-k_1(E,J)[t_r+t_2]}]e^{-k_2[B]t_r} \quad (12)$$

Hence, the metastable to main beam intensity ratio is

$$\frac{i_{MS}(E,J,t_r)}{i_{MB}(E,J,t_r)} = \frac{F_{MS}(E,J,t_r)}{F_S(E,J,t_r) + F_D(E,J,t_r)} \quad (13)$$

This equation must be averaged over the E and J distributions of the nascent collision complex obtained from the thermal flux through the orbiting transition state; hence

$$\frac{i_{MS}(t_r)}{i_{MS}(t_r)} = \int_0^\infty dE\, e^{-E/k_BT}\int_0^{J_{max}} dJ\, 2JF^{orb}(E,J)F_{MS}(E,J,t_r)/$$
$$\int_0^\infty dE\, e^{-E/k_BT}\int_0^{J_{max}} dJ\, 2JF^{orb}(E,J)F_S(E,J,t_r) +$$
$$\int_0^\infty dE e^{-E/k_BT}\int_0^{J_{max}} dJ\, 2JF^{orb}(E,J)F_D(E,J,t_r) \quad (14)$$

Finally, eq 14 should be averaged over the distribution of times that the nascent complex would spend in the ion source in the absence of unimolecular reaction. This distribution is not accessible experimentally. The residence time distribution, which is measured experimentally, samples clusters that have been collisionally stabilized in the ion source as well as nascent clusters which are stable long enough to reach the detector, and also reflects the kinetics of nascent cluster ion formation. However, assuming that the measured residence time distribution approximates the required time distribution, eq 14 was averaged over the measured residence time distribution:

$$\frac{i_{MS}}{i_{MB}} = \frac{\int_0^\infty dt_r\, P(t_r)i_{MS}(t_r)}{\int_0^\infty dt_r\, P(t_r)i_{MB}(t_r)} \quad (15)$$

The calculated metastable to main beam intensity ratios are shown in Figures 1a, 1b, and 1c as the solid lines. Clearly, good agreement exists between theory and experiment for all the systems studied. Since the theory assumes single collision stabilization of the nascent clusters, it is tempting to interpret the good agreement between theory and experiment as indicating that stabilization efficiencies of near unity operate in these systems. However, trial calculations indicated that the calculated metastable to main beam intensity ratio was sensitive to the time distribution used. Since there is some uncertainty as to how well the measured residence time distribution approximates the required time distribution, the possibility exists that the good agreement between experiment and theory could be fortuitous. However, it is unlikely that such good agreement would be found for all three systems if the agreement were fortuitous. Taken together, the good agreement between experiment and theory assuming unit stabilization and the pressure independence of the kinetic energy release distributions, provide reasonably conclusive evidence that near unit stabilization efficiencies operate in these systems.

2. Kinetic Energy release Distributions. Assuming that the kinetic energy release is governed by the orbiting transition state and that one collision is sufficient to stabilize the nascent complex, the probability of kinetic energy release E_t is:

$$P(E_t) =$$
$$\int_0^\infty dE\, e^{-E/k_BT}\int_0^{J_{max}} dJ\, 2JF^{orb}(E,J)P_\tau(E,J,t_r)P(E,J,E_t)/$$
$$\int_0^\infty dE e^{-E/k_BT}\int_0^{J_{max}} dJ\, 2JF^{orb}(E,J)P_\tau(E,J,t_r) \quad (16)$$

where $P_\tau(E,J,t_r)$ is the fraction of nascent complexes that dissociate in the second field-free region:

$$P_\tau(E,J,t_r) = \exp[-k_1(E,J)(t_1 + t_r)] - \exp[-k_1(E,J)(t_2 + t_r)] \quad (17)$$

Equation 16 should be averaged over the distribution of the time that nascent complexes spend in the ion source in the absence of unimolecular reactions. Since this is not accessible experimentally, averaging was performed over the measured ion source residence time distribution. Trial calculations indicated that the calculated kinetic energy release distributions were insensitive to the residence time. For example, for $H_2O{\cdot}H_3O^+$ increasing the residence time from 4 to 20 μs reduced the average kinetic energy release by 4%.

The results of the calculations are shown in Figures 2a, 2b, and 2c as the solid lines. The experimental data are shown as the points. The calculated kinetic energy release for the decomposition of $CO_2{\cdot}CO_2^{+}{\cdot}$ is slightly less than the experiment, and for $H_2O{\cdot}H_3O^+$ and $NH_3{\cdot}NH_4^+$ the calculated release is significantly larger than experiment. The agreement between experiment and theory is much better for $CO_2{\cdot}CO_2^{+}{\cdot}$ than for $H_2O{\cdot}H_3O^+$ and $NH_3{\cdot}NH_4^+$. The phase space calculations reported here employ the ion-induced dipole potential:

$$V(r) = -q^2\alpha/2r^4 \quad (18)$$

This potential is likely to be a relatively good approximation for $CO_2{\cdot}CO_2^{+}{\cdot}$. However, for $NH_3{\cdot}NH_4^+$ and $H_2O{\cdot}H_3O^+$ the neutral products both possess permanent dipole moments. Hence, the long-range potential in these systems is more realistically represented by the ion–dipole potential[34,35]

$$V(r) = -\frac{q^2\alpha}{2r^4} - \frac{\mu_D q}{r^2}\cos\theta \quad (19)$$

Including this potential into the phase space volume calculations is not a trivial problem. We are currently developing the required computer programs, however, in order to determine if the more attractive potential is the cause of the discrepancy found for $H_2O{\cdot}H_3O^+$ and $NH_3{\cdot}NH_4^+$. Some trial calculations were performed using an increased polarizability in the ion-induced dipole potential. The increased polarizability will make the ion-induced dipole potential more attractive. Some of the results of these calculations are shown in Figures 2a and 2b as the dashed lines. Clearly, much better agreement experiment and theory exists using the modified potential. The values of the polarizabilities used in the calculations shown in Figures 2a and 2b were values which, when used to calculate the ion-induced dipole capture rate constant, give the same rate constant as that calculated from average dipole orientation (ADO) theory.[34,35]

The improved agreement between experiment and theory using the modified potential suggests that the cause of the original discrepancy between experiment and theory occurred because the ion-induced dipole potential used in the theory is not sufficiently attractive for systems which also have a permanent dipole moment. However, a question remains concerning the validity of simply increasing the polarizability. The added term varies as r^{-2} (not r^{-4}) and hence will contribute differently to the potential in the region of the centrifugal barrier than a potential obtained simply by increasing α in eq 16.

Increasing the polarizability in the calculations of the metastable to main beam intensity ratio was found to have only a minor effect:

(34) T. Su and M. T. Bowers, *J. Chem. Phys.*, **58**, 3027 (1973).
(35) T. Su and M. T. Bowers, in "Gas Phase Ion Chemistry", Vol. I., M. T. Bowers, Ed., Academic Press, New York, 1979.

Table II. Summary of the Input Parameters Used in the Phase Space Calculations of $NH_3 \cdot NH_4^+$

	$NH_4^+ + NH_3$	$N_2H_7^+$
ν_i/cm^{-1} [a]	3100 (4)	3000 (6)
	1685 (2)	1676
	1397 (3)	1578 (4)
	3400 (3)	1434 (2)
	1628 (2)	954 (4)
	950	668
		105 (2)
B_1/cm^{-1} [b]	5.865	0.7302
B_2/cm^{-1} [b]	8.359	
B_{INT}/cm^{-1} [b]		11.73
σ [c]	36	18
E^+/eV [d]	1.041	
$\alpha/Å^3$ [e]	2.145	
μ/amu [f]	8.743	
K_{ADO}^{183} [g]	2.51×10^{-9} cm^3 s^{-1}	

[a] Vibrational frequencies in cm^{-1}. [b] Rotational constants in cm^{-1}; B_{INT} is the rotational constant for free rotation about the N···H···N bond. [c] Rotational symmetry number. [d] Zero-point energy difference in eV. [e] Polarizability of neutral in $Å^3$. [f] Reduced mass in amu. [g] ADO capture rate constant at 183 K (ref 34 and 35).

Table III. Summary of the Input Parameters Used in the Phase Space Calculations for $H_2O \cdot H_3O^+$ [a]

	$H_3O^+ + H_2O$	$H_2O \cdot H_3O^+$
ν_i/cm^{-1}	3660	3100 (2)
	1595	2800 (2)
	3760	1500 (2)
	3330	1050 (4)
	900	1000
	3150 (2)	670
	1615 (2)	180 (2)
B_1/cm^{-1}	15.58	0.8205
B_2/cm^{-1}	9.334	
B_{INT}/cm^{-1}		6.501
σ	6	8
E^+/eV	1.357	
$\alpha/Å^3$	1.45	
μ/amu	9.2432	
K_{ADO}^{283}	2.29×10^{-9} cm^3 s^{-1}	
ΔS°_{exptl} [39] [b]	-102.5 J K^{-1} mol^{-1}	
ΔS°_{calcd} [c]	-102.7 J K^{-1} mol^{-1}	

[a] Parameters are as defined for Table II. [b] Measured value of ΔS° from equilibrium studies (ref 39). [c] Calculated value of ΔS° using the parameters in this table.

the ratio was reduced by less than 5%. Changing the polarizability changes the E and J distribution functions (inspect eq 14) as well as the rate constants $k(E,J)$. Clearly these effects must largely cancel. For the calculated kinetic energy release distributions, changing the polarizability results in changes in the distribution of E and J states which fragment in the experimental time window. We found that increasing the polarizability shifts the J distribution of the metastable reactants to lower J. This change in the J distribution alone favors the formation of products with lower kinetic energy (due to the operation of conservation of angular momentum restrictions). Hence, the changes in the kinetic energy release distributions arising from changing the polarizability are not only due to changes in energy partitioning, but are also due to changes in the E and J distributions of the metastable reactants.

IV. Conclusions

The good agreement between experiment and theory supports the hypothesis that the observed metastables are statistical in nature (rather than due to a rotational or electronic predissociation). The lack of an ion source pressure dependence for the measured kinetic energy release distributions suggests that a single collision between the nascent complex and a neutral is sufficient to deactivate the complexes below their dissociation threshold. This experimental result is strongly supported by the theoretical model developed for the metastable to main beam intensity ratio wherein it is assumed that a single collision quenches the metastable fragmentation. These results, therefore, present direct evidence for the single collision stabilization assumption which is often made when dealing with ion–molecule association reactions stabilized by the parent gas.[1-5]

Table IV. Summary of the Input Parameters Used in the Phase Space Calculations for $CO_2 \cdot CO_2^{+\cdot}$ [a]

	$CO_2^{+\cdot} + CO_2$	$CO_2 \cdot CO_2^{+\cdot}$
ν_i/cm^{-1}	1388	1350 (2)
	667 (2)	580 (4)
	2349	1900 (2)
	1280	200
	498 (2)	120
	1469	50 (2)
B_1/cm^{-1}	0.3804	0.15
B_2/cm^{-1}	0.3902	
σ	4	4
$E^\ddagger/eV$	0.681	
$\alpha/Å^3$	2.59	
μ/amu	22.0	
K_{Lang} [b]	8.04×10^{-10} cm^3 s^{-1}	
ΔS°_{exptl} [5]	-95.4 J K^{-1} mol^{-1}	
ΔS°_{calcd}	-95.4 J K^{-1} mol^{-1}	

[a] Parameters are as defined in Tables II and III. [b] Langevin capture rate constant (ref 35).

The modeling of the kinetic energy release distribution demonstrates how inadequate the ion–induced dipole potential may be for calculating these quantities when applied to systems with a permanent dipole moment. In this work the neutral polarizability was increased to make the potential more attractive. This resulted in good agreement between theory and experiment. More work is planned in this area to develop a more rigorous theoretical model that explicitly includes molecular dipole moments.

Acknowledgment. We gratefully acknowledge the U. S. Air Force Office of Scientific Research (AFOSR) for support of this research through Grant AFOSR82-0035. We also thank the National Science Foundation (Grant CHE80-20464) and the donors of the Petroleum Research Fund administered by the American Chemical Society (Grant 12008-AC5-6) for partial support of this research. One of us (M.F.J.) acknowledges the Science and Research Engineering Council (U.K.) for a NATO/SERC Fellowship held during part of this work.

V. Appendix

The parameters used in the calculations are summarized in Tables II to IV. Parameters for the ammonia system were taken from the previous work of Bass et al.[29] For the water system, the vibrational frequencies and rotational constants of H_3O^+ and H_2O were taken from the work of Clair and McMahon.[36] Ab initio calculations[37] for the proton-bound dimer $H_2O \cdot H_3O^+$ indicate that the D_{2d} structure is the most stable. The rotational constant for $H_2O \cdot H_3O^+$ was calculated using structural information from these calculations. We have assumed that free rotation exists about the O···H···O bond and have calculated the internal rotational constant using structural information from the ab initio calculations. For the preceding parameters, values were either known or could be reliably estimated. The remaining parameters required were the vibrational frequencies of $H_2O \cdot H_3O^+$. There are limited experimental data on some of the vibrational frequencies of $H_2O \cdot H_3O^+$ from IR and Raman studies of crystals.[38] A set of frequencies was estimated using these data and frequencies for similar modes in other molecules. This set of frequencies was then

(36) R. Clair and T. B. McMahon, *Int. J. Mass. Spectrom. Ion Phys.*, **39**, 27 (1981).
(37) M. D. Newton and S. Ehrenson, *J. Am. Chem. Soc.*, **93**, 4971 (1971); P. A. Kollman and L. C. Allen, *ibid.*, **92**, 6101 (1970).
(38) G. Zundel, "Hydration and Intermolecular Interaction", Academic Press, New York, 1969; D. Hadzi and S. Bratos in "The Hydrogen Bond", P. Schuster, G. Zundel, and C. Sandorfy, Eds. North-Holland, Amsterdam, 1976.

refined by adjusting the frequencies so that the entropy change for the reaction

$$H_2O{\cdot}H_3O^+ \rightleftharpoons H_3O^+ + H_2O \qquad (A\text{-}1)$$

calculated using statistical thermodynamics matched the measured ΔS from equilibrium studies.[39] Finally the zero-point energy differences between $H_2O{\cdot}H_3O^+$ and $H_3O^+ + H_2O$ was calculated using statistical thermodynamics from known heats of formation,[40] the proton affinity of H_2O,[41] and the ΔH of reaction A-1 from equilibrium studies.[39]

Parameters for the CO_2 system were evaluated in a similar way to those for the water system. Vibrational frequencies and rotational constants of $CO_2^+\cdot$ and CO_2 are available from spectroscopic studies.[42] Since we could find no experimental or theoretical information on the structure of $CO_2{\cdot}CO_2^+\cdot$, we assumed that the CO_2 moieties are parallel with a C–C distance of 2 Å to calculate the rotational constant. The vibrational frequencies of $CO_2{\cdot}CO_2^+\cdot$ and the zero-point energy difference were evaluated as described above for $H_2O{\cdot}H_3O^+$ using the ΔS and ΔH recently measured by Headley et al.[5]

For $H_2O{\cdot}H_3O^+$ and $CO_2{\cdot}CO_2^+\cdot$ there are several reported measurements of ΔH and ΔS.[5,39,43,44] The ΔH values agree within 10%. The ΔS values show a larger scatter. Since the ΔS values were used to refine the vibrational frequencies of the complexes, some trial calculations were performed for $H_2O{\cdot}H_3O^+$ with the vibrational frequencies raised and lowered by 20% to determine how sensitive the calculations were to these parameters. Changing the vibrational frequencies over a range of 40% (which corresponds to a range in ΔS of 20%) resulted in a change of less than 20% in the calculated average kinetic energy release. The calculated average kinetic energy release increased as the vibrational frequencies were lowered. These changes could not account for the discrepancy between experiment and theory in the $H_2O{\cdot}H_3O^+$ systems, but changes of this magnitude could account for the smaller differences found between experiment and theory in the $CO_2{\cdot}CO_2^+\cdot$ system. For a 40% change in the vibrational frequencies the calculated metastable to main beam intensity ratio changed by a factor of approximately 2. The intensity ratio increased as the vibrational frequencies were lowered. Since in Figure 2 the log of the intensity ratio is plotted, changing the vibrational frequencies in the calculations is reflected as a relatively small offset to the calculated lines. This does not affect our conclusions regarding the operation of rear unit stabilization efficiencies in these systems. The calculated line is much more sensitive to the stabilization efficiency; reducing the stabilization efficiency to 0.5 results in nearly an order of magnitude increase in the calculated intensity ratio.

Registry No. $H_2O{\cdot}H_3O^+$, 22206-74-2; $NH_3{\cdot}NH_4^+$, 56044-48-5; $CO_2{\cdot}CO_2^+$, 12693-15-1.

(39) A. J. Cunningham, J. D. Payzant, and P. Kebarle, *J. Am. Chem. Soc.*, **94**, 7627 (1972).
(40) H. M. Rosenstock, K. Draxl, B. W. Steiner, and J. T. Herron, *J. Phys. Chem. Ref. Data*, **6**, (1977), Suppl. No. 1 (Energetics of Gaseous Ions); "JANAF Thermochemical Tables", 2nd ed., National Bureau of Standards, Washington, D.C. 1971, NSRDS-NBS37.
(41) R. Walder and J. L. Franklin, *Int. J. Mass Spectrom. Ion Phys.*, **36**, 85 (1980).
(42) D. Gauyacq, M. Horani, S. Leach, and J. Rostas, *Can. J. Phys.*, *53*, 2040 (1975), and references therein.
(43) M. Maut-Ner and F. H. Field, *J. Chem. Phys.*, **66**, 4527 (1977).
(44) P. Kebarle, S. K. Searles, A. Zolla, J. Scarborough, and M. Arshadi, *J. Am. Chem. Soc.*, **89**, 6393 (1967).

Sonochemistry and Sonocatalysis of Metal Carbonyls

Kenneth S. Suslick,* James W. Goodale, Paul F. Schubert, and Hau H. Wang

Contribution from the School of Chemical Sciences, University of Illinois at Urbana-Champaign, Urbana, Illinois 61801. *Received February 10, 1983*

Abstract: Ultrasonic irradiation of liquids produces acoustic cavitation: the rapid formation, growth, and implosive collapse of vapor filled vacuoles. This generates short-lived "hot spots" with peak temperatures ~3000 K and nanosecond lifetimes. We have studied the effects of high intensity ultrasound on a variety of metal carbonyls and have observed the general phenomenon of sonochemical ligand dissociation, which often produces multiple CO substitution. $Fe(CO)_5$, for example, upon sonolysis, yields $Fe_3(CO)_{12}$ in the absence of additional ligands and $Fe(CO)_3L_2$ and $Fe(CO)_4L$ (L = phosphine or phosphite) in their presence. Similar substitution patterns are observed for $Fe_3(CO)_{12}$, $Mn_2(CO)_{10}$, $Cr(CO)_6$, $Mo(CO)_6$, and $W(CO)_6$. In all cases examined the rates of sonochemical ligand substitution are first order in metal carbonyl concentration and independent of L concentration. In addition, $\ln K_{obsd}$ correlates well with solvent system vapor pressure. These results are consistent with a dissociative mechanism in which coordinatively unsaturated species are produced by the cavitation process. Further use of these transient intermediates is made as alkene isomerization catalysts. Sonocatalysis by a wide range of metal carbonyls shows many similarities to photocatalysis, but different relative efficiencies and selectivities have also been observed.

The chemical effects of high intensity ultrasound arise from acoustic cavitation of liquids:[1] this rapid formation, growth, and implosive collapse of gas vacuoles generates short-lived (~ns), localized "hot spots" whose peak temperatures and pressures have been measured at ~3000 K and ~300 atm,[2] confirming earlier calculations.[3] Analogies to flash pyrolysis, photochemistry, radiolysis, and other high-energy processes can be made. A resurgence of interest in the chemical uses of ultrasound in homogeneous[4,5] and heterogeneous[6] systems may be noted. We

(1) (a) El'piner, I. E. "Ultrasound: Physical, Chemical and Biological Effects"; Trans. F. L. Sinclair, Consultants Bureau, New York, 1964. (b) Margulis, M. A. *Russ. J. Phys. Chem. (Engl. Transl.)* **1976**, *50*, 1. (c) Apfel, R. E. "Methods in Experimental Physics"; Edmonds, P., Ed.; Academic Press: New York, 1981; Vol. 19.
(2) Sehgal, C.; Steer, R. P.; Sutherland, R. G.; Verrall, R. E. *J. Chem. Phys.* **1979**, *70*, 2242.
(3) Neppiras, E. A. *Phys. Rep.* **1980**, *61*, 159 and references therein.
(4) (a) Suslick, K. S.; Schubert, P. F.; Goodale, J. W. *J. Am. Chem. Soc.* **1981**, *103*, 7342. (b) Suslick, K. S.; Schubert, P. F.; Goodale, J. W. *Ultrason. Symp. Proc.* **1981**, 612. (c) Suslick, K. S.; Gawienowski, J. J.; Schubert, P. F.; Wang, H. H. *J. Phys. Chem.* **1983**, *87*, 2299. (d) Suslick, K. S.; Schubert, P. F. *J. Am. Chem. Soc.*, in press.
(5) (a) Lorimer, J. P.; Mason, T. J. *J. Chem. Soc., Chem. Commun.* **1980**, 1135. (b) Margulis, M. A. *Khim. Zhizn* **1981**, 57. (c) Nishikawa, S.; Otani, U.; Mashima, M. *Bull. Chem. Soc. Jpn.* **1977**, *50*, 1716. (d) Makino, K.; Mossoba, M. M.; Riesz, P. *J. Am. Chem. Soc.* **1982**, *104*, 3537. (e) Rosenthal, I.; Mossoba, M. M.; Riesz, P. *J. Magn. Reson.* **1981**, *45*, 359. (f) Yu, T. J.; Sutherland, R. G.; Verrall, R. E. *Can. J. Chem.* **1980**, *58*, 1909. (g) Sehgal, C.; Sutherland, R. G.; Verrall, R. E. *J. Phys. Chem.* **1980**, *84*, 2920. (h) Sehgal, C.; Yu, T. J.; Sutherland, R. G.; Verrall, R. E. *Ibid.* **1982**, *868* 2982. (i) Sehgal, C. M.; Wang, S. Y. *J. Am. Chem. Soc.* **1981**, *103*, 6606. (j) Staas, W. H.; Spurlock, L. A. *J. Chem. Soc., Perkin Trans. 1* **1975**, 1675.

0002-7863/83/1505-5781$01.50/0